Research Article Vol. 1, No. 4 / 15 Apr 2022 / Optics Continuum 747
OPTICS CONTINUUM

Thin-disk multipass amplifier delivering sub-400 fs pulses with excellent beam quality at an average power of 1 kW

André Loescher,[1,*] Florian Bienert,[1] Christoph Röcker,[1] Thomas Graf,[1] Martin Gorjan,[2] Jürg Aus der Au,[2] and Marwan Abdou Ahmed[1]

[1] Universität Stuttgart, Institut für Strahlwerkzeuge (IFSW), Pfaffenwaldring 43, 70569 Stuttgart, Germany
[2] Spectra-Physics, MKS Instruments, Inc., Feldgut 9, 6830 Rankweil, Austria
[*] andre.loescher@ifsw.uni-stuttgart.de

Abstract: We present an improved multipass amplifier design, enabling the amplification of ultrashort pulses with excellent beam quality to more than 1 kW of average output power. 260 fs short pulses at an average power of 105 W and a repetition rate of 1 MHz were directly amplified up to an average power of 1033 W. The pulse duration at this power level was measured to be 388 fs assuming a Gaussian temporal shape. This corresponds to a peak power of 2.5 GW. The power stability was measured to be 0.16% RMS over a duration of more than two hours at a sampling rate of 2 Hz. High beam quality is proven with measured values of M_x^2 = 1.16 in the horizontal and M_y^2 = 1.19 in the vertical plane according to ISO Standard 11146.

1. Introduction

Ultrafast lasers have become essential for many fields of material processing such as precise ablation, drilling of deep holes, or surface structuring [1–3]. Depending on the application, different values of parameters such as wavelength, pulse duration, repetition rate, and pulse energy are required [4–7]. Either way, all applications require stable lasers in terms of beam pointing, output power, and beam quality. Besides a small beam propagation factor M^2 also a symmetric intensity distribution along the whole caustic, as well as high stigmatism is often of importance for applications. Since the direct generation of ultrashort pulses at high average power and with high pulse energy with all these properties is not an easy task, laser amplifiers are commonly used. These can be designed in different ways. Fiber amplifiers, for example, are known to provide high beam quality and low intensity noise, both being a consequence of their underlying architecture, i.e. the fiber-optic beam guiding. On the downside, however, ultrafast fiber lasers are limited by the nonlinearities occurring due to the high intensities and the long interaction length in the fibers. Hence, techniques such as divided pulse amplification (DPA), chirped pulse amplification (CPA), and coherent beam combination (CBC) are applied to handle high peak powers in fibers [8]. To date, the highest average power reported for ultrafast lasers is 10.4 kW with 0.13 mJ of energy per pulse and a pulse duration of 254 fs which was achieved by CPA and CBC of 12 individual amplifiers [9]. A higher pulse energy of 12 mJ at an average power of 700 W and a pulse duration of 262 fs was achieved exploiting CBC of 8 single amplifiers together with DPA and CPA [8]. Both fiber-based systems delivered pulses with a near-diffraction limited beam quality of $M^2 < 1.2$.

In contrast to fiber lasers, thin-disk lasers are capable of handling much higher peak power and pulse energies, thanks to the large beam diameter and the short interaction length in the active medium. Up to 200 mJ of pulse energy were demonstrated with a CPA-based regenerative amplifier containing two thin laser disks [10]. This system delivered 1.1 ps short pulses at an average power of 1421 W with a beam propagation factor of $M^2 < 1.2$. Increasing the repetition

#451490 https://doi.org/10.1364/OPTCON.451490
Journal © 2022 Received 15 Dec 2021; revised 9 Feb 2022; accepted 9 Feb 2022; published 1 Apr 2022

OPTICS CONTINUUM

rate to 20 kHz enabled the extraction of 1.95 kW of average output power while the pulse duration and beam propagation factor were measured to be 800 fs and $M^2 < 1.4$, respectively [11].

Regenerative amplifiers however lack flexibility in terms of adaptable repetition rates. This flexibility can be accessed using thin-disk multipass amplifiers (TDMPAs) since they support a wide range of repetition rates as well as continuous wave operation. This concept is based on the geometrical folding of the beam path over a thin-disk laser medium. This passive concept enables scaling of power and pulse energy to the kilowatt and millijoule level, respectively, without the mandatory need of CPA. The TDMPA architecture is suitable for pulse durations ranging from femtoseconds to nanoseconds as well as pulse bursts and continuous wave operation [12–15]. Recently, 2 kW of average power were demonstrated with 6.8 mJ of pulse energy and a pulse duration of 7.7 ps [16]. A similar average power of 1.9 kW was obtained from a more compact multipass amplifier generating pulses with 4.8 mJ of energy a duration of 1.3 ps [17]. The reported beam propagation factors however depended on the output power and were measured to be $M^2 = 1.5$ [16] and $M^2 = 2.3$ [17] at maximum power. Short pulses with a duration of 260 fs were amplified up to an average power of 528 W and 0.4 mJ of pulse energy with the system reported in Ref. [12]. Here, the beam propagation factor was measured to be $M^2 = 1.24$. Using a more powerful seed laser this amplifier delivered 560 fs short pulses with an average power of 1 kW and 1 mJ of energy per pulse with a measured beam propagation factor of $M^2 = 1.5$ [18]. Using CPA, a multipass amplifier comprising 4 thin disks was used to amplify incident pulses with an energy of 240 mJ to an output pulse energy of 720 mJ, yielding 720 W of average power and a pulse duration of 920 fs. The beam propagation factor was however measured to be approx. $M^2 = 2.1$ [19]. In the present paper we report on an improved CPA-free multipass amplifier system delivering sub-400 fs pulses with up to 1 kW of average power and 1 mJ of pulse energy. In contrast to previous TDMPAs, the output beam quality ($M^2 < 1.2$) as well as the intensity distribution were almost unaffected by the amplification process.

2. Investigation of the main challenges in TDMPA systems

By carefully analyzing our previous systems [12,16,20,21] we identified three main causes affecting the overall performance concerning output power and beam quality. These were temperature gradients in the amplifier's atmosphere (i.e. locally heated air inside the pump module), thermally induced deformation of opto-mechanical components leading to power-dependent drifts, and wavefront distortions introduced by the mounting of optical components. Since one key point of the TDMPAs is the amplification of laser radiation to a high power level of several hundreds of watts or beyond, the usage of high-power pump sources is mandatory. High pumping intensities in turn lead to high temperatures in the gain medium as well as in the ambient gas. This brings along additional challenges such as the formation of thermal- and gas-lenses, air-wedges, and beam pointing fluctuations due to gas turbulences [22,23]. These problems are detrimental for TDMPAs because of their long beam path and also since the beam passes the disk and thus the disturbances in the nearby atmosphere multiple times. A strong air wedge in front of the disk may even lead to a walk-off of the laser beam out of the pumped area. One way to reduce the effect of the air wedge on the propagating laser beam is the implementation of a so called retro-reflecting mirror pair (RMP) [20]. While air turbulences usually cause periodic movement of the laser beam, thermally induced deformation of the mechanical components lead to slow drifts. These thermally induced drifts of the opto-mechanical components might also cause a walk-off of the seeded beams out of the pumped area on the laser disk. This would cause a reduction of the extraction efficiency and induce diffraction of the amplified beam. Another reason for the degradation of the beam quality and the symmetry of the intensity distribution originates from surface distortions of the employed optics. These distortions can either be intrinsic to the optics themselves or they can be stress-induced by the mechanical mounts as the thermal expansion of the mounts increases the stress applied to the optical components. This

OPTICS CONTINUUM

provokes the distortion to be temperature dependent and thus depends both on the laser power and the thermalisation time of the mounting mechanics.

3. Setup and improvements

In order to address the challenges described above and to further optimize the TDMPA, improvements of key components were carried out without changing the TDMPA's main concept. These improvements as well as the whole setup is described in this section.

The TDMPA presented in this work is based on the concept reported in [20]. The experimental setup is sketched in Fig. 1. The seed laser emitted 260 fs short pulses with a repetition rate of 1 MHz at an average power of 105 W. The spectrum was centered at a wavelength of 1030.5 nm and the beam propagation factor was M^2 = 1.11 in both the horizontal and the vertical plane. In a first step, the seed beam was collimated to a diameter of 4.5 mm (D4σ) using a mirror telescope and subsequently guided into the TDMPA. A 125 µm thin Yb:YAG disk with a diameter of 20 mm and a doping concentration of 10–11 at. % was used as gain medium. The disk was pumped at the zero-phonon line at a wavelength of 969 nm by a fiber-coupled diode delivering a maximum pump power of 1.8 kW. The disk was mounted in a 24-pass pumping cavity and the diameter of the pump spot was 5.4 mm (FWHM). In order to fold the seed beam 40 times over the disk, a mirror array composed of 80 adjustable mirrors was implemented. It was placed at a distance of 1.2 m from the disk and used in a single-pass configuration, where the pulses were guided through the complete TDMPA only once. The frame of the mirror array as well as the optical breadboard of the amplifier were made of temperature-controlled aluminum. By this, the system was stable for several months without the need of realignment.

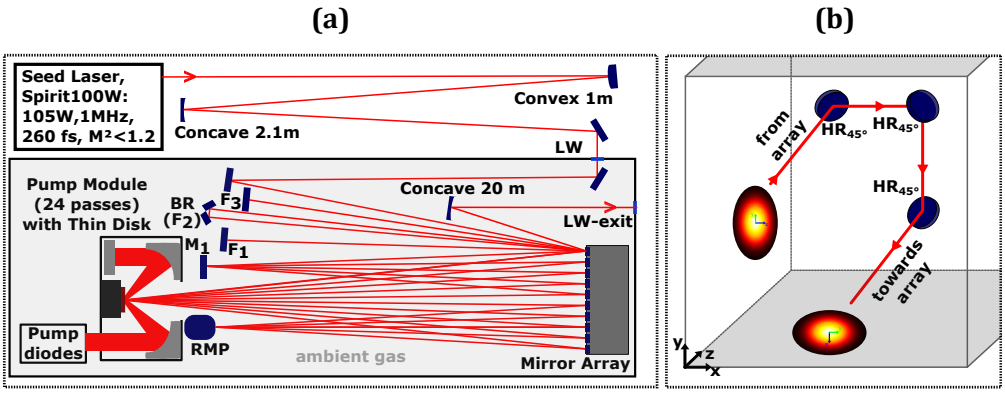

Fig. 1. (a) Top view of the setup of the thin-disk multipass amplifier (a). The beam rotator (BR) consists of three high-reflective (HR) 45°-folding mirrors (b). LW: Laser window, F1-3: folding mirror 1-3, BR: beam rotator, RMP: retro-reflecting mirror pair.

Until now, the TDMPAs were set up with plane folding mirrors at the locations labeled M1, F1, F2, and F3 in Fig. 1(a). These mirrors were used to guide the laser beam to the different lines of the mirror array. In order to enhance the symmetry of the intensity distribution of the output beam, the beam rotator (BR) was implemented as a new element to replace the mirror at F2, which has the advantage that the influence of asymmetric optical elements of the TDMPA on the propagating beam is minimized. With this measure, the beam leaving the TDMPA is highly symmetric even when optical elements of the amplifier exhibit asymmetric curvatures. Further improvements aiming at minimizing distortions of the optical elements and diminishing thermally induced pointing fluctuations of the laser beam compared to previously developed TDMPAs were achieved by a mechanical redesign of the mount of mirror M1, a new geometry of

OPTICS CONTINUUM

the mirrors used in the mirror array, and the addition of helium to the ambient gas inside the TDMPA, as explained in the following.

1. Opto-mechanics:

As described in section 2, TDMPAs are rather sensitive to thermal drifts of the opto-mechanical components and distortions introduced by optical elements due to the long beam path. Depending on the design, the length of the beam path typically ranges between 100 m and 250 m. Besides this long propagation distance, the beam is subjected to multiple reflections at different optical elements. The amplifying thin disk and the folding mirror M1 are particularly critical, since they affect 40 and 20 reflections of the beam, respectively. Their mechanical design and cooling were therefore improved accordingly. For the mirror M1 a new mirror mount which presses the mirror with its rear side onto a cooled heat sink by means of a spring on the front of the mirror was developed. This axial clamping approach was chosen since all radial mounting approaches led to distortions of the mirror's surface. The spring as well as all components involved in the holding of the mirror are shielded against stray light to suppress thermally induced surface deformations and drifts. The mirror array was also redesigned under this aspect by using special mirrors, incorporating a knop on their backside, enabling to isolate all the mechanics behind the mirror's apertures from stray light as sketched in Fig. 2. The mirror has a monolithic geometry with two concentric cylinders of different diameters. The front facet of the large cylinder was HR-coated to act as the mirror. The cylinder located at the backside is used for the mechanical mounting to the kinematic mirror mount. This technique has the additional advantage that the clamping of the mirror can hardly introduce any distortions of the mirror surface on the front. The mirror rear side with the smaller diameter is clamped inside a mirror mount, which in turn is attached to the water-cooled mirror array. The mount's kinematic is protected against stray light originating from the pump module since the diameter of the mechanical mount is smaller than the diameter of the mirror's HR-coated front surface.

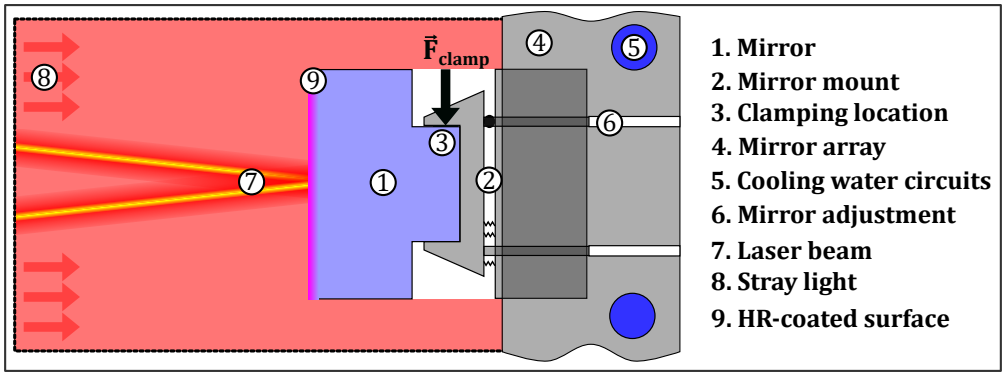

Fig. 2. Side view of one mirror mounted in the water-cooled mirror array. The mount's kinematic is protected against stray light by the larger HR-coated front surface of the mirror. The access to alignment is enabled through openings in the base plate of the mirror array.

2. Ambient gas:

Typical temperatures of the surface in the pumped area of the thin disk range between 80 °C and 120 °C during laser operation. This leads to thermally induced natural convection of the surrounding gas as well as to the formation of a gas lens in front of the disk, which can negatively affect the amplification process. As described in section 2, the effect of the tilt induced to the

OPTICS CONTINUUM

laser beam by the "air wedge" next to the disk is already commonly diminished by means of the RMP. To further minimize this effect as well as the impact of natural convection, we operated the presented system in a helium atmosphere at normal pressure of 1 bar, as the temperature dependence dn/dT of the refractive index of helium is lower than the one of air [22]. Hence, temperature gradients in the ambient gas cause lower fluctuations of the beam pointing as well as reduced positional displacements, which is crucial for instance in the pumped region of the thin disk.

3. Beam propagation:

Since the beam repeatedly passes the thin disk and the central folding mirror M1, any intrinsic imperfections of these two parts add up with the number of beam passes and may lead to significant distortions of the beam's intensity profile. In the propagation scheme described in [20,21], all optical components except for the thin disk are chosen to be plane. When the RoC of the thin disk differs in the horizontal and vertical direction, astigmatism is caused in the amplified beam. We observed that the change of the RoC of the disk can be caused by both the mounting

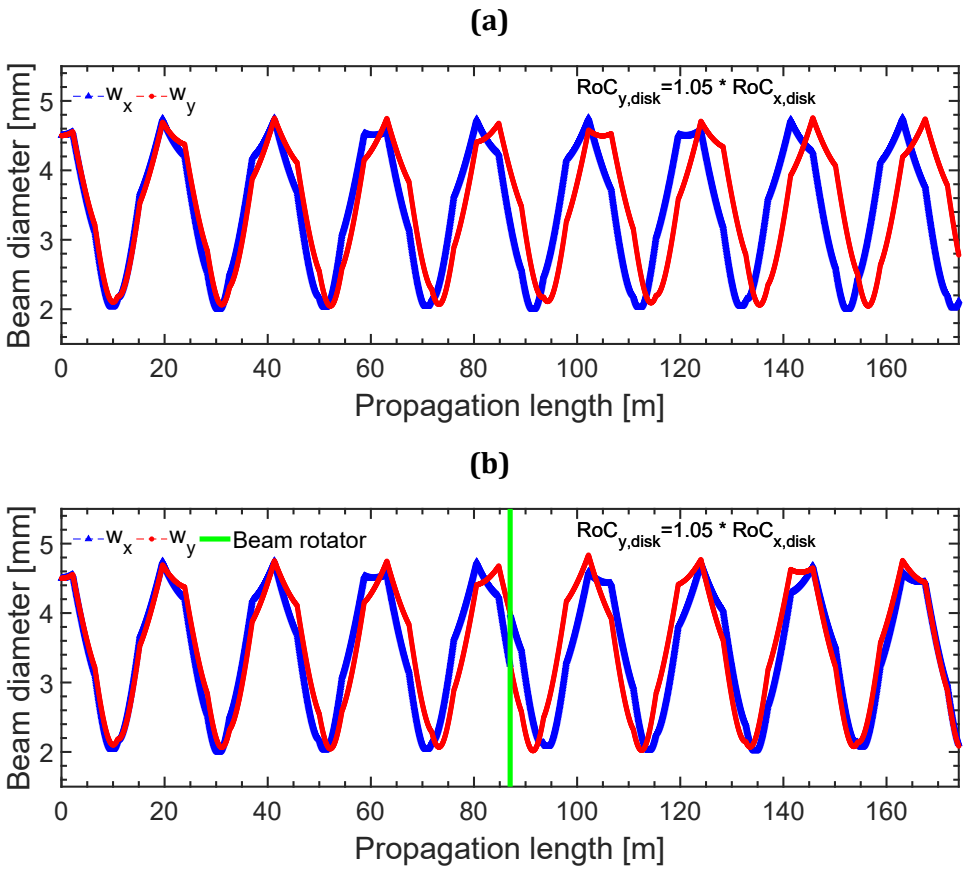

Fig. 3. Calculated beam caustic in the TDMPA without (a) and with (b) beam rotator. A collimated beam with a diameter of 4.5 mm is launched into the system. The thin disk is the only curved element with a radius of curvature (RoC) of 20 m. The RoC in the vertical direction (y-axis) is larger than in the horizontal direction (x-axis) by a factor of 1.05 (≈ 21 m). The beam rotator was located after the 20th reflection at the disk, corresponding to half of the propagation distance as indicated by the green line.

OPTICS CONTINUUM

and the amplification process. On the one hand, a high clamping torque on the diamond induces an uncontrolled deformation of the thin disk, which is glued on the diamond heat sink. On the other hand, high-power pumping leads to a temperature rise in the pumped region of the disk and consequently to thermo-optical and thermo-mechanical deformations [22,24,25]. We identified the difference between the RoC in the horizontal (x) and the vertical (y) plane with respect to the optical table to be the main contribution to the distortion occurring in our systems. This is illustrated by calculations of the corresponding beam diameters along the propagation path through the amplifier for the exemplary case with $RoC_y = 1.05 \cdot RoC_x$ shown in Fig. 3(a) when no BR is implemented. It can be seen that the beam diameters in the horizontal and vertical planes start to differ significantly after a propagation length of approx. 60 m. Figure 3(a) shows the calculated ratio d_x/d_y of the beam diameters in the horizontal (x) and vertical (y) plane and the ratio θ_x/θ_y of the divergences as a function of the ratio RoC_y/RoC_x of the disk's RoC in the horizontal and vertical planes when no BR is implemented. The RoC_y ranges from 19 m to 21 m, whereas RoC_x is kept constant with a value of 20 m. As expected, the optimum fully stigmatic output beam is only obtained with $RoC_y/RoC_x = 1$. Within the considered range of RoC_y the astigmatism has a maximum when the ratio RoC_y/RoC_x is 0.95, hence $RoC_y = 19$ m. The effects of the asymmetric curvatures of the disk, which cannot easily be controlled directly, can be reduced by rotating the beam in order to symmetrize the suffered distortions. To this end a BR composed of three mirrors, see Fig. 1(b), forming an off-angle periscope was introduced in the present setup and was found to significantly improve the optical performance as compared to previously presented TDMPAs. As indicated by the simulations shown in Fig. 3(b) the image-rotation results in a more symmetric and stigmatic output beam. Figure 3(b) shows the calculated beam diameter with the same parameters as used in Fig. 3(a), but with the BR implemented. As it can be seen, the beam diameters d_x and d_y are nearly equal at the output of the system. The astigmatism that is accumulated in the first half of the beam is compensated for by the second half of the path because of the rotation introduced by the BR in the middle of the path (at approx. 87 m from the start). Figure 4(b) shows the output beam parameters for different RoC_y/RoC_x values when the BR is implemented. Here, the output beam's ellipticity and astigmatism are strongly reduced over the whole range, which confirms that the BR has a significant beneficial influence on the symmetry of the output beam.

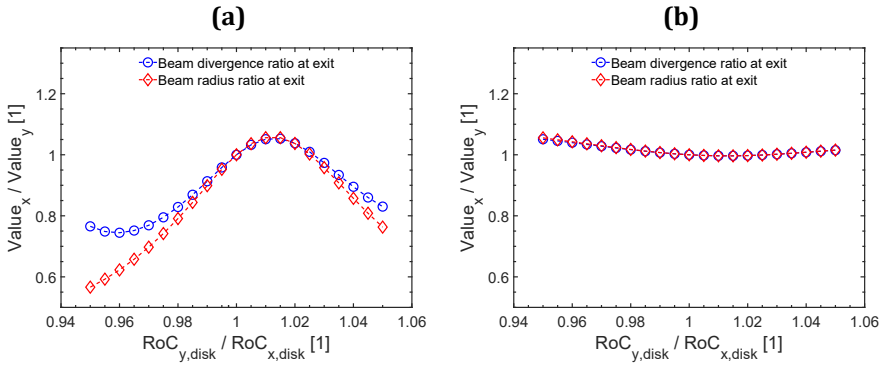

Fig. 4. Simulated ratio of the output beam's diameter and divergence for different astigmatism of the disk without (a) and with the beam rotation (b).

4. Experimental results

The measured average output power and calculated extraction efficiency obtained with the optimized TDMPA design are shown in Fig. 5 as a function of the pump power. The extraction

OPTICS CONTINUUM

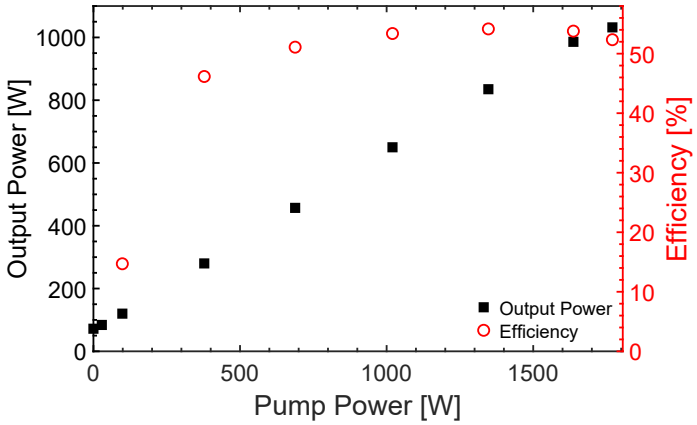

Fig. 5. Average output power and extraction efficiency (seed power of 105 W subtracted) of the amplified beam as a function of the pump power launched into the pump module.

efficiency corresponds to the average output power with the seed power being subtracted divided by the pump power launched into the thin-disk pumping module. When no pump power was applied, part of the seed power of 105 W was absorbed in the disk resulting in a measured output power of 72 W after 40 reflections on the disk. At maximum pump power of 1770 W launched into the pumping module an output power of 1033 W was obtained, corresponding to an extraction efficiency of 52.4%. The maximum extraction efficiency of 54.2% was reached at a pump power of 1350 W. The temporal and spectral properties of the ultrashort pulses were analyzed by means of a commercial autocorrelator (pulseLink, APE) and spectrometer (HR4000, OceanOptics), respectively. The measured autocorrelation traces and spectra are presented in Fig. 6. For best agreement with the measured trace, we assumed a Gaussian temporal shape for the amplified pulses and sech^2 temporal shape for the pulses, which were not amplified. The difference in the autocorrelation traces of the seed pulses propagated through the amplifier without amplification and the amplified pulses at maximum average power is clearly visible in Fig. 6(a). The pulse duration increased from 268 fs to 388 fs. This increase by 120 fs is mainly attributed to the

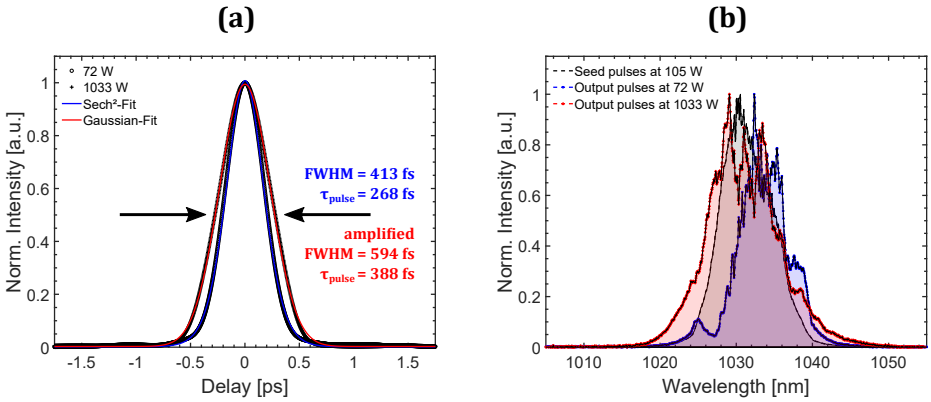

Fig. 6. (a) AC-trace of the pulses at the average powers of 72 W and 1033 W. (b) Spectra of the seed pulses (black line), at 72 W of average output power (blue line), and at 1033 W of average power (red line).

OPTICS CONTINUUM

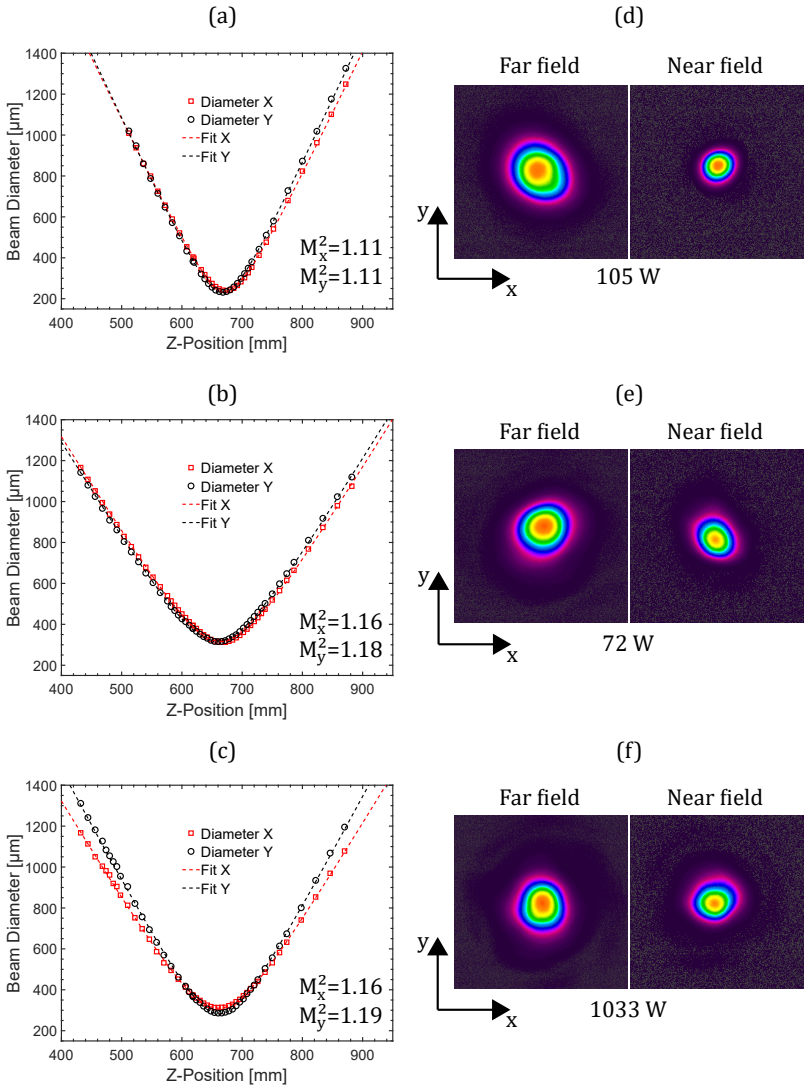

Fig. 7. Caustic of the seeded laser beam before injection into the TDMPA at 105 W of average power (a), and after propagation through the unpumped TDMPA at 72 W of transmitted average power (b), and of the amplified laser beam at 1033 W of average power (c). Far- and near-field intensity profiles of the seeded beam (d), of the seeded beam propagated through the unpumped TDMPA (e), and of the amplified beam at 1033 W of average power (f).

influence of dispersion and self-phase modulation, which is visible by comparing the spectral intensity of the amplified and seeded laser pulses shown in Fig. 6(b). The spectra of the seeded laser pulses, the seeded laser pulses after transmission through the unpumped TDMPA, and the amplified laser pulses at the maximum power of 1033 W are represented by a black-colored, blue-colored, and green-colored line, respectively. At this maximum power level, the spectral bandwidth (FWHM) increased by 5 nm to 12 nm with respect to the seeded laser pulse. This yields that an approximately three times shorter pulse duration of 130 fs would be supported by this spectral bandwidth of the amplified pulses, offering the possibility for subsequent pulse

OPTICS CONTINUUM

compression as reported e.g. in Ref. [26]. In order to obtain transform-limited pulses, the amount of required group delay dispersion (GDD) was calculated to be -17200 fs^2. Furthermore, we estimated the accumulated B-integral to be 4 and 17.5 rad for the case where the amplifier is filled with helium and air, respectively. The calculations are based on the modulated beam size depicted in Fig. 3 and we assumed an amplification of up to 1 kW of average power. One advantage of the used "quasi-collimated beam" propagation scheme over the approach of the 4f-propagation scheme is the prevention of tight foci inside the amplifier. For the laser powers applied in our work, a 4f-propagation would lead to values of the B-integral of 5 and 34.7 rad when the amplifier is filled with helium and air, respectively. In addition to a relatively high B-integral, the 4f-propagation scheme is quite sensitive to misalignments and thermal lensing of the thin disk.

The key aspect of our TDMPA was the preservation of the beam propagation factor and the symmetry of the intensity distribution of the amplified beam. Those were measured according to ISO Standard 11146 by means of a commercial analyzer (BeamSquared, Ophir Optronics). The amplified beam at maximum output power exhibited an excellent beam propagation factor of $M_x^2 = 1.16$ in the horizontal and $M_y^2 = 1.19$ in the vertical direction, very close to those of the seed beam with $M_{x,y}^2 = 1.11$ when propagated through the unpumped TDMPA, which results in a beam propagation factor of $M_x^2 = 1.16$ and $M_y^2 = 1.18$. The measured caustics are shown in Fig. 7(a-c). The corresponding intensity profiles in the far and near field are presented in Fig. 7(d-f). By comparing the intensity profiles shown in Fig. 7(e) and 7(f) it can be concluded that the output beam was not distorted, neither in the far nor in the near field. Considering the ISO-compliant measurements, these results represent, to the best of our knowledge, the highest beam quality achieved at these average and peak power for thin-disk based multipass amplifiers.

The beam propagation factor was also analyzed in dependence of the average output power. The result is summarized in Fig. 8, which shows that the measured M^2 value remained below 1.2 over the complete range of output power. By comparing M_y^2 and M_x^2 one finds that the M^2 was slightly higher in the vertical (y) direction. These minor differences in beam quality are suspected to arise from slight residual pump power dependent misalignment of the beam path in the TDMPA.

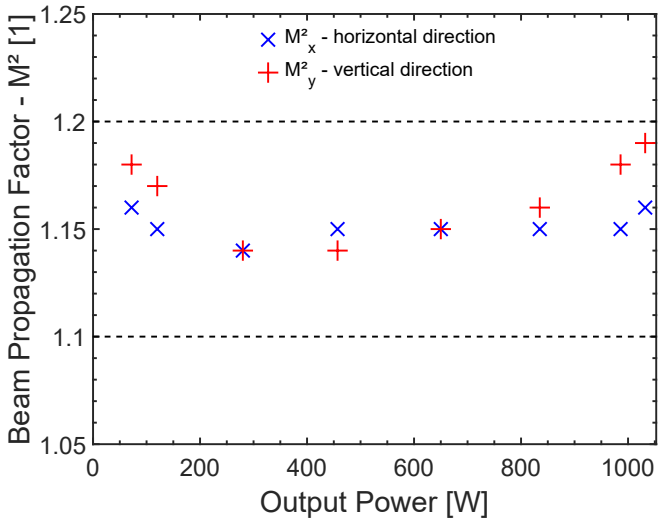

Fig. 8. Beam propagation factor measured as function of output power.

OPTICS CONTINUUM

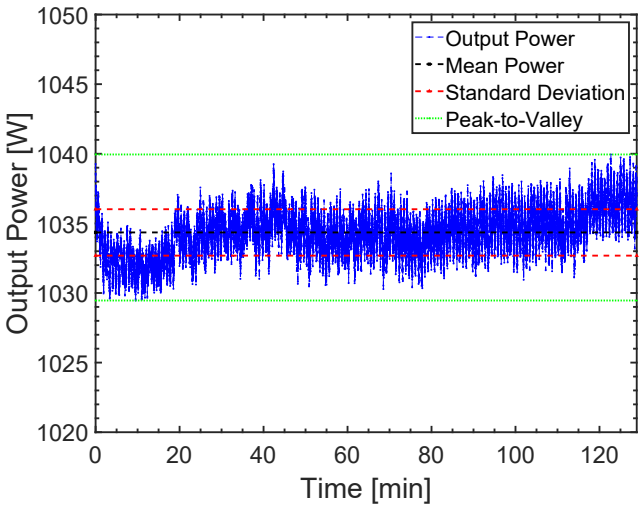

Fig. 9. Average output power as a function of the time at 1770 W of pump power.

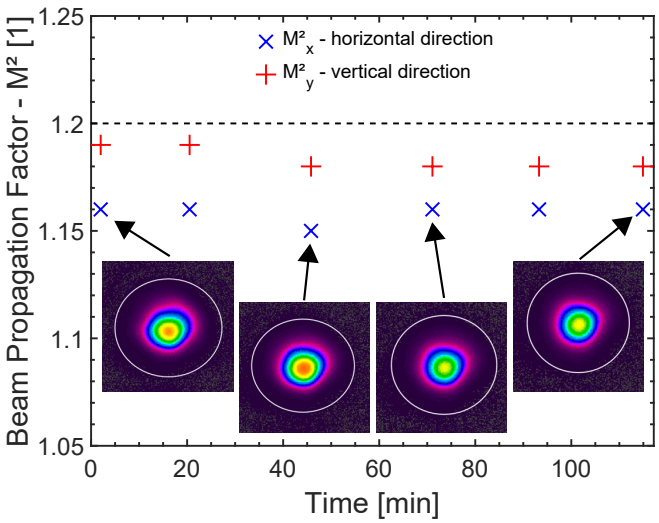

Fig. 10. Beam propagation factor in dependence of the time at constant pump power of 1770 W. The insets show the intensity profiles in the near field.

OPTICS CONTINUUM

The beam propagation factor was also analyzed in dependence of the average output power. The result is summarized in Fig. 8, which shows that the measured M^2 value remained below 1.2 over the complete range of output power. By comparing M_y^2 and M_x^2 one finds that the M^2 was slightly higher in the vertical (y) direction. These minor differences in beam quality are suspected to arise from slight residual pump power dependent misalignment of the beam path in the TDMPA.

A measurement of the long-term stability of the power and the beam propagation factor at maximum output power are shown in Fig. 9 and Fig. 10, respectively. The amplifier system was operated at a constant pump power of 1770 W during more than 2 hours for this analysis. The mean value, standard deviation (STD), and the peak-to-valley (PtV) deviation are inserted as horizontal lines in black, red, and green, respectively, in Fig. 9. The mean value was found to be 1034.4 W with a STD of 1.7 W, which shows a high power stability of RMS < 0.2% (2 Hz sampling rate). In the same duration of 2 h, the PtV was 10.5 W corresponding to a maximum relative deviation of 1%. During this experiment, the beam propagation factor was measured approx. every 20 minutes as summarized in Fig. 10. Four insets show the intensity distribution in the near field after operation for 2, 45, 70, and 120 minutes. The M^2 was less than 1.2 during the whole time and increased only by 1.25% at maximum power. It is worth mentioning that no feedback loop was implemented to stabilize neither the power nor the alignment of the amplifier.

5. Conclusion and outlook

To summarize we presented a TDMPA system capable to directly amplify sub-300 fs pulses up to an average power of 1 kW with excellent beam quality. At a pump power of 1.77 kW 388 fs short pulses with an average power of 1033 W were generated. The beam propagation factor was less than 1.2 in all measurements. In addition, the long-term measurement showed a high power stability of RMS < 0.2% for two hours of operation. These performances were achieved thanks to an optimized optical layout comprising a beam rotator (BR), improved mounting of the main folding mirror (M1), as well as and optimized design of the mirrors in the mirror array to minimize stress-induced distortions. Furthermore, helium at atmospheric pressure was used as ambient gas to reduce the air-wedge and gas-lens effect occurring next to the pumped thin disk. Future investigations will focus on further power scaling using a more powerful pump source. Estimations indicate that close to 2 kW of average output power can be achieved with this system by increasing the pump power to 4 kW and the diameter of the pump spot to 8 mm. Scaling the pulse energy to several tens of millijoules will require to increase the beam sizes on the optics, since the typical damage threshold of coatings is in the range of 0.5–1 J/cm^2 for pulse durations below 1 ps. We expect that CPA has to be adapted when the pulse peak power exceeds 2 to 4 GW, in order to prevent critical self-focusing. Furthermore, the influence of different concentrations of helium in the ambient gas on the output pulses will be studied in more detail.

Funding. Horizon 2020 Framework Programme (825246).

Acknowledgements. This project is an initiative of the Photonics Public Private Partnership from the European Union's Horizon 2020 research and innovation programme under grant agreement No 825246.

Disclosures. The authors declare no conflicts of interest.

Data availability. Data underlying the results presented in this paper are not publicly available at this time but may be obtained from the authors upon reasonable request.

References

1. C. Momma, S. Nolte, B. N. Chichkov, F. V. Alvensleben, and A. Tünnermann, "Precise laser ablation with ultrashort pulses," Appl. Surf. Sci. **109-110**, 15–19 (1997).
2. D. J. Förster, R. Weber, D. Holder, and T. Graf, "Estimation of the depth limit for percussion drilling with picosecond laser pulses," Opt. Express **26**(9), 11546 (2018).
3. D. Holder, R. Weber, C. Röcker, G. Kunz, D. Bruneel, M. Delaigue, T. Graf, and M. A. Ahmed, "High-quality high-throughput silicon laser milling using a 1 kW sub-picosecond laser," Opt. Lett. **46**(2), 384 (2021).

OPTICS CONTINUUM

4. A. Feuer, C. Kunz, M. Kraus, V. Onuseit, R. Weber, T. Graf, D. Ingildeev, and F. Hermanutz, "Influence of laser parameters on quality of microholes and process efficiency," Laser Appl. Microelectron. Optoelectron. Manuf. XIX **8967**, 89670H (2014).
5. M. Jenne, D. Flamm, T. Ouaj, J. Hellstern, J. Kleiner, D. Grossmann, M. Koschig, M. Kaiser, M. Kumkar, and S. Nolte, "High-quality tailored-edge cleaving using aberration-corrected Bessel-like beams," Opt. Lett. **43**(13), 3164 (2018).
6. S. Faas, U. Bielke, R. Weber, and T. Graf, "Scaling the productivity of laser structuring processes using picosecond laser pulses at average powers of up to 420 W to produce superhydrophobic surfaces on stainless steel AISI 316L," Sci. Rep. **9**(1), 1933 (2019).
7. B. Neuenschwander, B. Jaeggi, M. Schmid, and G. Hennig, "Surface structuring with ultra-short laser pulses: Basics, limitations and needs for high throughput," Phys. Procedia **56**, 1047–1058 (2014).
8. M. Kienel, M. Müller, A. Klenke, J. Limpert, and A. Tünnermann, "12 mJ kW-class ultrafast fiber laser system using multidimensional coherent pulse addition," Opt. Lett. **41**(14), 3343 (2016).
9. M. Müller, C. Aleshire, A. Klenke, E. Haddad, F. Légaré, A. Tünnermann, and J. Limpert, "10.4 kW coherently combined ultrafast fiber laser," Opt. Lett. **45**(11), 3083 (2020).
10. T. Nubbemeyer, M. Kaumanns, M. Ueffing, M. Gorjan, A. Alismail, H. Fattahi, J. Brons, O. Pronin, H. G. Barros, Z. Major, T. Metzger, D. Sutter, and F. Krausz, "1 kW, 200 mJ picosecond thin-disk laser system," Opt. Lett. **42**(7), 1381 (2017).
11. C. Wandt, C. Herkommer, R. Jung, S. Klingebiel, P. Krötz, S. Prinz, M. Rampp, C. Y. Teisset, K. Michel, and T. Metzger, "Ultrafast thin-disk based CPA system with > 1 kW output power and < 500 fs pulse duration," *Opt. InfoBase Conf. Pap. 2020*, 3–4 (2020).
12. C. Röcker, A. Loescher, J.-P. Negel, M. Delaigue, F. Morin, C. Hönninger, E. Mottay, P. Villeval, A. Holvoet, D. Lupinski, T. Graf, and M. Abdou Ahmed, "Direct amplification of sub-300 fs pulses in a versatile thin-disk multipass amplifier," Opt. Commun. **460**, 125159 (2020).
13. A. Antognini, K. Schuhmann, F. D. Amaro, F. Biraben, A. Dax, A. Giesen, T. Graf, T. W. Hänsch, P. Indelicato, L. Julien, C. Y. Kao, P. E. Knowles, F. Kottmann, E. Le Bigot, Y. W. Liu, L. Ludhova, N. Moschüring, F. Mulhauser, T. Nebel, F. Nez, P. Rabinowitz, C. Schwob, D. Taqqu, and R. Pohl, "Thin-disk Yb:YAG oscillator-amplifier laser, ASE and effective Yb: YAG lifetime," IEEE J. Quantum Electron. **45**(8), 993–1005 (2009).
14. M. Schulz, R. Riedel, A. Willner, S. Düsterer, M. J. Prandolini, J. Feldhaus, B. Faatz, J. Rossbach, M. Drescher, and F. Tavella, "Pulsed operation of a high average power Yb:YAG thin-disk multipass amplifier," Opt. Express **20**(5), 5038 (2012).
15. S. Nagel, B. Metzger, D. Bauer, J. Dominik, T. Gottwald, V. Kuhn, A. Killi, T. Dekorsy, and S. Schad, "Thin-disk laser system operating above 10 kW at near fundamental mode beam quality," Opt. Lett. **46**(5), 965 (2021).
16. C. Röcker, A. Loescher, F. Bienert, P. Villeval, D. Lupinski, D. Bauer, A. Killi, T. Graf, and M. Abdou Ahmed, "Ultrafast green thin-disk laser exceeding 1.4 kW of average power," Opt. Lett. **45**(19), 5522 (2020).
17. T. Dietz, M. Jenne, D. Bauer, M. Scharun, D. Sutter, and A. Killi, "Ultrafast thin-disk multi-pass amplifier system providing 1.9 kW of average output power and pulse energies in the 10 mJ range at 1 ps of pulse duration for glass-cleaving applications," Opt. Express **28**(8), 11415 (2020).
18. C. Röcker, A. Loescher, M. Delaigue, C. Hönninger, E. Mottay, T. Graf, and M. A. Ahmed, "Flexible sub-1 ps ultrafast laser exceeding 1 kW of output power for high-throughput surface structuring," *Adv. Solid State Lasers - Proc. Laser Congr. 2019 (ASSL, LAC, LS C) 2019*, 4–5 (2019).
19. C. Herkommer, P. Krötz, R. Jung, S. Klingebiel, C. Wandt, R. Bessing, P. Walch, T. Produit, K. Michel, D. Bauer, R. Kienberger, and T. Metzger, "Ultrafast thin-disk multipass amplifier with 720 mJ operating at kilohertz repetition rate for applications in atmospheric research," Opt. Express **28**(20), 30164 (2020).
20. J.-P. Negel, A. Voss, M. A. Ahmed, D. Bauer, D. Sutter, A. Killi, and T. Graf, "1.1 kW average output power from a thin-disk multipass amplifier for ultrashort laser pulses," Opt. Lett. **38**(24), 5442 (2013).
21. J.-P. Negel, A. Loescher, A. Voss, D. Bauer, D. Sutter, A. Killi, M. A. Ahmed, and T. Graf, "Ultrafast thin-disk multipass laser amplifier delivering 1.4 kW (4.7 mJ, 1030 nm) average power converted to 820 W at 515 nm and 234 W at 343 nm," Opt. Express **23**(16), 21064 (2015).
22. A. Diebold, F. Saltarelli, I. J. Graumann, C. J. Saraceno, C. R. Phillips, and U. Keller, "Gas-lens effect in kW-class thin-disk lasers," Opt. Express **26**(10), 12648 (2018).
23. T. Dietrich, C. Röcker, T. Graf, and M. Abdou Ahmed, "Modelling of natural convection in thin-disk lasers," Appl. Phys. B **126**(3), 47 (2020).
24. A. Giesen, H. Hügel, A. Voss, K. Wittig, U. Brauch, and H. Opower, "Scalable concept for diode-pumped high-power solid-state lasers," Appl. Phys. B **58**(5), 365–372 (1994).
25. A. Voss, M. Abdou Ahmed, C. Neugebauer, A. Giesen, and T. Graf, "Intracavity beam shaping for high power thin-disk lasers," in *XVI International Symposium on Gas Flow, Chemical Lasers, and High-Power Lasers* (2006), Vol. 6346, p. 63461U.
26. B. Dannecker, J. P. Negel, A. Loescher, P. Oldorf, S. Reichel, R. Peters, T. Graf, and M. Abdou Ahmed, "Exploiting nonlinear spectral broadening in a 400 W Yb:YAG thin-disk multipass amplifier to achieve 2 mJ pulses with sub-150 fs duration," Opt. Commun. **429**, 180 (2018).